DRAG DUE TO REGULAR ARRAYS OF ROUGHNESS ELEMENTS OF VARYING GEOMETRY*

R. A. WOODING[a], E. F. BRADLEY[b], and J. K. MARSHALL[c]

(Received 8 August, 1972)

Abstract. Comparisons are made of experimental studies on the drag, at high Reynolds number, due to regular arrays of roughness elements of various shapes immersed in a turbulent boundary layer. Using a variant of Millikan's dimensional analysis, the form of the velocity profile is deduced in terms of the dimensions and concentration of the roughness elements. A drag formula results which is shown to be in good agreement with data. Available measurements of the partition of drag between the elements and the intervening surface indicates that equipartition occurs at quite low concentrations. The interaction between elements is then small, so that the drag coefficient of a typical roughness element is nearly constant.

A re-examination of some of O'Loughlin's velocity-profile data, obtained below the tops of the roughness elements, suggests the existence of a nearly constant-stress layer scaled to the shear stress of the intervening surface. Above the roughness elements, the mean-velocity profile undergoes a transition to the form appropriate to the total shear stress exerted by the roughened surface. A formula is given which describes the one-dimensional velocity profile over the entire range, excluding the viscous sublayer on the intervening surface. The viscous sublayer appears to correspond quite closely to that on a smooth plate.

Notation

ROUGHNESS GEOMETRY AND DISTRIBUTION

A_r frontal area of roughness element
D distance between rows of roughness elements and transverse distance between individual elements
L length scale depending on k, d, s and D (Equation (4))
S specific area or average area of flat surface per roughness element
S' that part of S not covered by the roughness element
d horizontal dimension of roughness element transverse to flow
k roughness height
k' length scale of Clauser (1956) in Equation (13)
k_s equivalent sand-grain roughness height of Nikuradse (1933)
m coalescing factor of Koloseus and Davidian (1966)
s horizontal dimension of roughness element parallel to flow
z vertical distance above test plate or intervening surface between roughness elements

* This work was initiated while the authors were with the Division of Plant Industry, CSIRO. Their present affiliations are:
[a] Applied Mathematics Division, D.S.I.R., Wellington, New Zealand.
[b] Division of Environmental Mechanics, CSIRO, Canberra, A.C.T. Australia.
[c] Rangelands Research Unit, CSIRO, Deniliquin, N.S.W., Australia; at present on leave at the Natural Resource Ecology Laboratory, Colorado State University, Fort Collins, Colorado, U.S.A.

Boundary-Layer Meteorology 5 (1973) 285–308.

AIRFLOW

A reciprocal von Karman's 'constant' $=1/\kappa$ (Table I)
A' constant in Equation (19)
C constant in Equations (8), (10), (11), (12), (17)
C' constant in Equation (19)
C_f roughness element drag coefficient (Equation (16))
F, G notation indicating functional dependence
K_m momentum diffusion coefficient
M limiting Reynolds number $=u_{*g}\delta_s/\nu$
U velocity at $z=\delta$
b length adjustment of lower and upper velocity profiles through the transition region
u mean horizontal velocity
u_k mean horizontal velocity at height k
u_s velocity at upper edge of viscous sublayer
u_* total shear velocity $=(\tau/\varrho)^{1/2}$
$\tilde{u}_*$ upstream wall shear velocity
u_{*g} mean shear velocity for uncovered surface
w_r mean drag per element

β constant introduced in Equation (9)
δ turbulent shear layer or boundary-layer thickness
δ_s smooth wall sublayer thickness
κ von Karman's 'constant'
λ roughness concentration $=A_r/S$
ν fluid kinematic viscosity
ϱ fluid density
τ total shearing stress
ϕ notation indicating functional dependence which, given certain assumptions, $\approx(k/s)^{\beta}$
χ, ψ notation transcribed from Sayre and Albertson (1961)

1. Introduction

Studies of flow over roughened surfaces have developed in two principal directions. An extensive literature exists for the first of these, which concerns the transition of a laminar boundary layer to turbulence and the influence of roughness in inducing transition. Reviews by Dryden (1953) and Tani (1961) may be mentioned in particular. The second direction of study, which is the topic of this paper, concerns the drag of roughened surfaces in a fully-developed turbulent shear flow, as in rough pipes or in the atmospheric boundary layer. In the case of total drag, a wide range of measurements exists, the most complete early work being Nikuradse's (1933) studies using

sand-roughened pipes. From this work has stemmed the concept of an 'equivalent sand-grain roughness height' k_s, which is the basis of the Von Karman-Prandtl resistance law valid at large Reynolds numbers. In any given situation, k_s is determined experimentally in terms of a measurable roughness dimension, usually the roughness height k, and the ratio k_s/k is then invariant for geometrically-similar roughness arrays. An early rough-wall boundary-layer description, not including k_s, was made by Corrsin and Kistler (1955).

Many drag problems involve surfaces quite unlike Nikuradse's sand-roughness. The drag on rivetted ship hulls led Schlichting (1936) to consider regular arrays of roughness elements of simple geometry, and in recent years this work has been extended considerably (e.g., Roberson, 1961, 1968; Roberson and Chen, 1970). For the parallel problem which exists in the lower atmosphere, Lettau (1967, 1969) has proposed a relationship between the aerodynamic roughness parameter z_0 and the geometry of the rough ground cover. Less attention has been given to the question of drag partition between the roughness elements and the intervening surface, which is an important factor in studies of soil erosion and of plant growth in partly vegetated areas (Marshall, 1970, 1971). It seems that this stress partition should also be dependent upon geometry.

2. Review of Experimental Studies

Table I summarizes roughness-element configurations used in a wide range of experiments.

Schlichting (1936) used a water tunnel, the working section consisting of two ducts, each of 4- by 17-cm cross-section and 320-cm length, joined end-to-end with the roughened test plate forming one of the wider walls in the downstream section. Thus the velocity profile at the entrance to the second section was already a partially-developed turbulent shear flow, characteristic of a two-dimensional smooth pipe.

The principal roughness arrays considered by Schlichting comprised transverse rows of elements distance D apart, with a distance D between rows. Successive rows were displaced laterally by $\frac{1}{2}D$ to give a 'diagonal' configuration. The main element shapes were spheres, spherical segments, truncated cones and short right-angled strips made from metal sheet of thickness 0.03 cm mounted transverse to the flow. He also made measurements with long strips extending across the test plate. For each configuration 5 or 6 measurements of total drag were made, varying the roughness Reynolds number over a range of at least 2:1.

Measurements with regular arrays of cubes have been reported by O'Loughlin and MacDonald (1964), and O'Loughlin (1965), who used both 'diagonal' and 'parallel' configurations. In the earlier study, the array covered an area 0.6×7.7 m on the floor of a tilting flume. The later study was performed in an air conduit of section 11.5×45.5 cm and 7.4 m long.

Moore (1951) carried out wind-tunnel studies using three arrays, 95 cm by 255 cm, composed of square bars mounted transversely to the flow, and spaced about 4 times the bar width. Moore gives the variation of total stress with distance downstream, so

TABLE I

Summary of experimental roughness-element parameters, with coefficients of straight lines fitted to total-drag data

Roughness element description	Roughness height k(cm)	k/s	k/d	Inverse of concentration $1/\lambda$ (range)	Fitted straight line (total drag) $U/u^* = A \ln(\delta/k\lambda\phi) + C$		Von Karman constant $\kappa = 1/A$	Reference
					A	C		
Spheres	0.41, 0.21	1	$= k/s$	6–95	2.40	0.79	0.42	Schlichting (1936)
Spherical segments	0.26	0.325	do	19–77	2.89	−1.69	0.35	
Truncated cones	0.375	0.47	do	13–53	3.32	−5.17	0.30	
Transverse short strips	0.30	10	0.375	16–67	3.06	−3.06	0.33	
Cubes	0.475	1	$= k/s$	64–256	3.41	−6.37	0.29	O'Loughlin (1965)
Above elements grouped					2.87	−2.05	0.35	
Cubes	0.475	1	$= k/s$	8–512	2.20	1.38	0.45	Koloseus and Davidian (1966)
Cylinders	2.54	0.2 to 2	do	18–1250	4.08	−5.25	0.25	Marshall (1971)
Hemispheres	2.54	0.5	do	25–480	4.14	−4.90	0.24	
Transverse long strips	0.3	10	0	6–18	–	–	–	Schlichting (1936)
Transverse square bars	0.317, 0.635	1	0	40–160	2.27	−3.56	0.44	Powell } See Koloseus and
	0.13	1	0	1.98	–	–	–	Chu *et al.* } Davidian (1966).
	3.86, 1.29, 0.32	1	0	3.95	1.61	7.30	0.62	Moore (1951)
	0.32	1	0	4	2.93	2.15	0.34	Antonia and Luxten (1971)
Vertical wires	7	23.3	$= k/s$	27.5	–	–	–	Bradley (1965)
Bushel baskets	30, 60	0.7, 1.4	do	3–384, 16	2.36	0.99	0.42	Kutzbach (1961)

that the effect of varying boundary-layer thickness δ can be observed. Recent drag studies, again using square bars, are reported by Antonia and Luxton (1971).

Bradley (1965, 1968) made surface drag and wind-profile measurements using an array of short vertical wires, the ratio k/d being very large, arranged in a square pattern on an airfield tarmac. The principal array dimensions were length 26 m and width 20 m. Bradley's results provide total-stress data with varying δ, as in Moore's experiments.

Kutzbach (1961) reported wind-profile experiments using arrays of bushel baskets arranged at various regular spacings in a 60° sector on lake ice, the maximum radius being 55 m. Values of the total shear velocity u_* were obtained from profile analysis.

None of this work was particularly concerned with the measurement of stress partition, although Schlichting made a few studies with a smooth test plate and Bradley (1965), by removing the roughness elements from the surface of the drag plate, showed that the surface stress within the array was close to 25% of the local value of total stress. O'Loughlin (1965) measured shear-stress ratios for several arrays of cubic elements. Einstein and Banks (1950) measured the change of drag in a flume caused by the addition of arrays of pegs, small transverse steps, or both together.

Marshall (1971) carried out wind-tunnel experiments to investigate the effect of changing roughness element shape and concentration (density), both on total stress and on partition of stress. The test plate, measuring 183 cm by 124 cm, was mounted in quite a short working section, 69 cm high, with the inlet end coupled to a 4:1 contraction. The roughness elements were vertical cylinders 2.54 cm high with k/d ratios of 2, 1, $\frac{1}{2}$, $\frac{1}{3}$ and $\frac{1}{5}$, and 2.54-cm diameter hemispherical elements. The spacing-height (D/k) ratios were varied from 2 to 50. The drag on individual roughness elements was measured directly as a function of downstream distance. Total drag measurements were made over the area of the test plate, using momentum budget and drag balance methods.

3. Total Drag – Theoretical

3.1. Dimensional considerations

In the geometrical description of a roughness array, the number of parameters which can be considered will not be adequate to specify the element shape and distribution completely. However, it is assumed here that the drag properties of an array are basically determined by a limited number of measurable parameters, for which a single approximate similarity relation to include different arrays may be applicable. Such a hypothesis is particularly plausible if the boundary-layer profiles are nearly similar for differing roughness geometries. In this paper, the approach is developed for regular arrays of roughness elements with finite horizontal dimensions ('three-dimensional' elements). The 'two-dimensional' case, e.g., that of long strips mounted transversely to the flow, has been discussed by Liu *et al.* (1966).

Classical dimensional analysis can be applied to the turbulent wall layer to take into account the role of relevant length and area scales associated with a roughness array. Let the z-axis be directed upwards. When the total wall stress is expressed in

terms of the shear velocity u_*, the law of the wall gives, for the profile of mean velocity u,

$$\frac{u}{u_*} = F\left[\frac{zu_*}{\nu}, \frac{z}{k}, \frac{z}{d}, \frac{z}{s}, \frac{z}{D}\right], \tag{1}$$

which is valid sufficiently close to the wall. Here F signifies an unknown function, ν is the kinematic viscosity, k is the roughness height, d and s are typical horizontal dimensions of the roughness elements with d transverse to, and s parallel to, the flow, while D is the mean element spacing (see Notation). In terms of the specific area S, or average area of horizontal surface per element, $D=S^{1/2}$ for 'three-dimensional' roughness elements. In the cases of most practical interest, when the roughness Reynolds number ku_*/ν is large, the argument zu_*/ν may be dropped from (1) for $z=\mathrm{O}(k)$ or greater.

In the outer region of the shear layer where $z=\mathrm{O}(\delta)$ (δ being the layer thickness), the velocity-defect law is

$$\frac{U-u}{u_*} = G\left[\frac{z}{\delta}, \cdots\right], \tag{2}$$

in which G is a second unknown function, and U is the velocity at $z=\delta$. For a growing boundary layer, δ is a function of x, the distance downstream from the beginning of the roughness array, and G may be a function of z/x also. This x-dependence is neglected for $\delta/x \ll 1$.

Strictly, F and G are representations of the same function, but are valid in different regions, subject to restrictions on the relative magnitudes of the parameters. Thus, F is independent of δ for $\delta/k \gg 1$. Again, G does not involve k, d, s and D provided that these quantities are small relative to δ. Care must be exercised in cases where $D \gg k$. As Schlichting (1936) showed using spherical roughness elements, the secondary-flow disturbances to the mean-velocity profile extend to a depth of order D in the shear flow. Hence it is necessary to assume that $\delta \gg D$, although not all of the experimental data satisfy that criterion.

Although F and G remain unknown functions, the possibility that there exists a region of overlap, in which both (1) and (2) are valid simultaneously, can be utilized to obtain asymptotic representations for that restricted range. This is a standard approach (Millikan, 1938; Coles, 1956), which is discussed in a modified form in the following paragraphs. The approach here is that of Landweber (Rouse, 1959), applicable to the case of a growing turbulent boundary layer, where the flow near $z=\delta$ depends upon upstream conditions for which the wall shear velocity, $\tilde{u}_*$, say, may differ from the local value u_*. It is necessary to eliminate $\tilde{u}_*$ so that only local 'independent' quantities occur. If there exists a region of overlap in the range $k<z<\delta$ where both (1) and (2) are valid, these equations can be added to give

$$\frac{U}{u_*} = F(z/k, z/d, z/s, z/D) + \frac{\tilde{u}_*}{u_*} G(z/\delta), \tag{3}$$

where both U/u_* and $\tilde{u}_*/u_*$ are functions of k, d, s, D and δ. Following Landweber, differentiation of (3) twice with respect to z and elimination of $\tilde{u}_*/u_*$ gives

$$\frac{z}{L}\frac{\mathrm{d}^2F}{\mathrm{d}(z/L)^2}\Big/\frac{\mathrm{d}F}{\mathrm{d}(z/L)} = \eta\frac{\mathrm{d}^2G}{\mathrm{d}\eta^2}\Big/\frac{\mathrm{d}G}{\mathrm{d}\eta}, \tag{4}$$

where $\eta = z/\delta$ and L is a length scale which depends upon k, d, s and D. Then, from the classical argument, each side of the equation must be a constant, which it will be convenient to denote by $\alpha - 1$.

When $\alpha = 0$, two integrations of either side of (4) lead to the logarithmic law. For $\alpha \neq 0$, integration of the right-hand side gives the power law

$$G \propto \eta^\alpha/\alpha + \text{constant}. \tag{5}$$

A similar expression can be obtained for F.

The constant α is also arbitrary. However, in the limiting case where $\tilde{u}_* = u_*$, the above classical argument can be applied after only one differentiation of (3), which then leads to the logarithmic law, i.e., $\alpha = 0$. It appears that α will be small for $\tilde{u}_*/u_*$ nearly equal to unity. An application of the well-known limit for natural logarithms

$$-\alpha^{-1}(\eta^{-\alpha} - 1) < \ln\eta < \alpha^{-1}(\eta^\alpha - 1)$$

shows that the difference between (5) and the logarithmic law is also small, for

$$\begin{aligned}\frac{1}{\alpha}(\eta^\alpha - 1) - \frac{1}{-\alpha}(\eta^{-\alpha} - 1) &= \frac{\eta^{-\alpha}}{\alpha}(\eta^\alpha - 1)^2 \\ &= O\{\alpha(\eta - 1)^2\},\end{aligned} \tag{6}$$

and $\eta - 1$ is small in the range of validity of G. It seems unlikely that the power law with a small parameter can be distinguished experimentally from a logarithmic law; the latter will be assumed to hold for $\tilde{u}_* \approx u_*$.

With this assumption, substitution for G in Equation (2) gives

$$\frac{U - u}{u_*} = \frac{1}{\kappa}\ln\frac{\delta}{z}, \tag{7}$$

where by convention, κ is von Karman's 'constant'.

A similar argument leads to a logarithmic form for the law of the wall involving the function F. It is then apparent from (1) and (7) that

$$\frac{u}{u_*} = F\left[\frac{z}{k}, \frac{zu_*}{\nu}, \frac{z}{d}, \frac{z}{s}, \frac{z}{D}\right] = \frac{1}{\kappa}\ln\frac{z}{L} + C\left[\frac{ku_*}{\nu}\right], \tag{8}$$

where C tends to a constant limit as $ku_*/\nu \to \infty$, the case assumed in this paper. It is apparent that the shear velocity u_* will depend upon the manner in which k, d, s and D are involved in the drag per unit area of the rough surface, and this same dependence must appear in L. If the element form drag is assumed dominant, the stress per unit area will be proportional to the concentration $\lambda = A_r/S$, i.e., to the ratio kd/D^2 when

the roughness-element shape is fixed qualitatively, e.g., cube, sphere, cone, etc. This simple picture is complicated by the fact that near the roughness elements, changes occur in the near-wake geometry with changes of element dimension in the flow direction. The data of Wieghardt (1953) and Tillmann (1953) indicate that the drag decreases with increasing s for $s/k = O(1)$, due to the reduction in volume of the separation bubble, where considerable dissipation occurs. Evidently an aspect-ratio factor $\phi(k/s, k/d)$ should be included, and experiments are necessary to determine its form. Unfortunately, except for the above two references, most experiments appear to have been made with symmetrical roughness elements for which $s = d$. Here a very simple assumption will be made that the dependence of ϕ upon k/d is small, and that the dependence upon k/s can be represented approximately, over a limited range, by the power law $\phi \approx (k/s)^{\beta}$, where β is a universal constant to be determined.

Then if the roughness height k is taken to determine the overall scale of the system,

$$L = k\lambda\phi \propto k\frac{kd}{D^2}\left(\frac{k}{s}\right)^{\beta}. \tag{9}$$

The law of the wall (8) then becomes

$$\frac{u}{u_*} = \frac{1}{\kappa}\ln\frac{z}{k\lambda\phi} + C, \tag{10}$$

and the drag law (3) reduces to

$$\frac{U}{u_*} = \frac{1}{\kappa}\ln\frac{\delta}{k\lambda\phi} + C. \tag{11}$$

A drag law closely resembling (11) has been developed empirically for cubic roughness elements by Koloseus and Davidian (1966) and compared with data by Schlichting and other authors. In their formula, L is replaced by $k\lambda^{\gamma}$, where the exponent γ varies from 0.9 (cubes) through 0.97 (spheres) to unity for several other forms of roughness element. Sayre and Albertson (1961) also developed a drag law in which L and C were combined in a roughness parameter with the dimension of length, $\chi = k\psi(\lambda)$, where ψ is determined empirically for each species of roughness.

3.2. Other representations for the total drag

Von Karman's (1934) formula

$$\frac{U}{u_*} = \frac{1}{\kappa}\ln\frac{\delta}{k_s} + \text{constant}$$
$$\approx 2.5\left(\ln\frac{\delta}{k_s} + 2.5\right)$$

for the drag of a rough plate makes use of the Nikuradse 'equivalent sand roughness' k_s as an empirical length to accommodate changes both in roughness scale and shape.

From (11), $\kappa \approx 0.4$ and

$$k_s \approx k\lambda\phi \exp(2.5 - 0.4C), \tag{12}$$

this result being valid in the range of validity of (11). Also, since the aerodynamic roughness parameter $z_0 \propto k_s$, a comparison can be made with Lettau's (1967, 1969) empirical formula $z_0 \approx 0.5\, k\lambda$.

Koloseus and Davidian (1966) have collected extensive data describing the variation of k_s with concentration λ; some of the data are summarized in Figure 1, definitions of terms being included in the caption. A 'coalescing factor' m, constant for a given

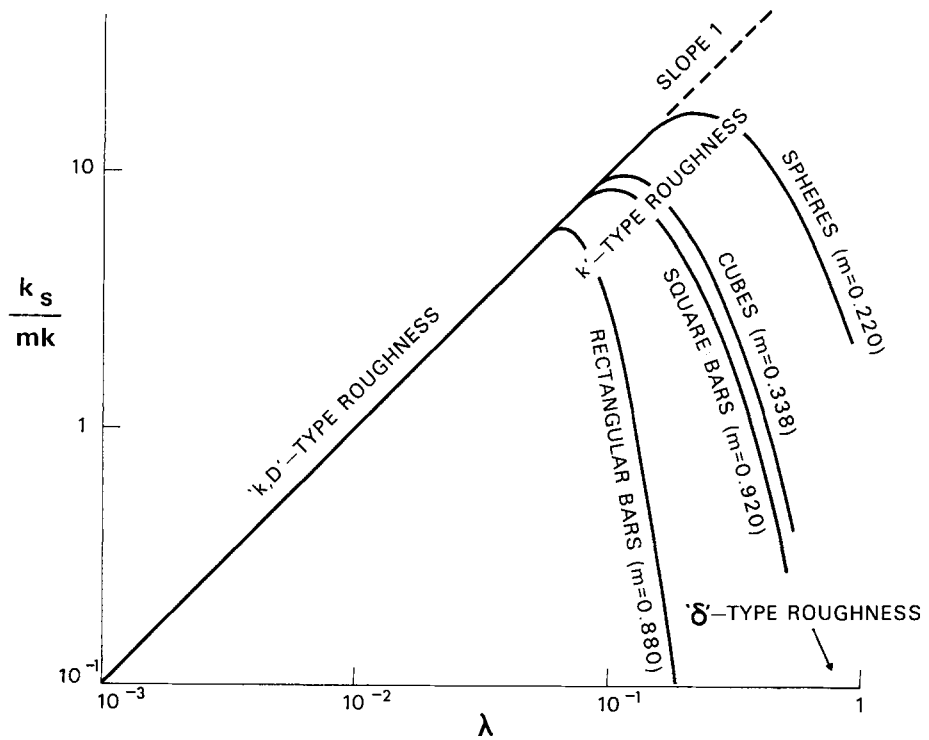

Fig. 1. Variation of equivalent roughness height with concentration of roughness elements (quoted from Koloseus and Davidian, 1966), indicating the approximate ranges of various 'roughness regimes'. Here roughness concentration λ = (frontal area per element)/(specific area), k_s is the equivalent sand-grain roughness height of Nikuradse (1933), and k is roughness height. The 'coalescing factor' m, introduced by Koloseus and Davidian, has been adjusted empirically to give unit slope in the straight-line range of the data.

shape of roughness element, has been introduced to bring the data for the low-concentration range on to a single straight line, of slope unity in agreement with (12).

The breakdown of (12), and therefore of (11) occurs when k_s/mk falls below this line with the onset of mutual sheltering at the higher values of λ (the initiation of 'skimming flow') (Morris, 1955). Perry *et al.* (1969) describe these λ-dependent regimes

as 'k'-roughness, and 'D'-roughness. Here, D stands for a pipe diameter. The analogous scale in our case is the boundary-layer thickness δ, and an appropriate designation would be 'δ'-roughness. In 'δ'-roughness, the space between adjacent roughness elements contains a stable eddy which aids in the establishment of 'skimming flow'. The shear layer above the elements is only slightly dependent on k, and is characterized by u_* and the thickness δ; for flat-topped roughness elements, the drag tends to the smooth-wall value as $\lambda \to 1$. For 'k'-roughness, the eddy between elements is unstable and is shed into the shear flow to give a turbulent structure scaled to the roughness height. Perry *et al.* (1969) envisage reverse flow at the smooth wall between elements in 'k'-roughness, which can hold only if the near-wake eddy of each element is large enough to fill the space, i.e., for $D = O(k)$. At small λ, re-attachment occurs between elements and the smooth wall makes a positive contribution to the total drag. This might be described as 'k, D'-roughness, when $D \gg k$, and the flow contains features depending upon both scales. Figure 1 indicates very approximately the range of each regime.

The rough-wall friction law proposed by Clauser (1956) envisages a vertical displacement of the smooth-wall profile by the presence of roughness:

$$\frac{U}{u_*} = \frac{1}{\kappa} \ln \frac{\delta u_*}{\nu} - \frac{\Delta u}{u_*} + \text{constant}, \tag{13}$$

where

$$\frac{\Delta u}{u_*} = \frac{1}{\kappa} \ln \frac{k' u_*}{\nu} + \text{constant}$$

is a measure of the shift. The form of (13) is determined by the fact that the inner law is independent of viscosity. According to Perry *et al.* (1969), the length k' is nearly proportional to k for 'k'-type roughness, and may be proportional to δ in the 'δ'-type. For 'k, D'-type roughness, reference to (11) indicates that

$$k' = k\lambda\phi \tag{14}$$

so that, for very small λ, $\Delta u/u_*$ is also small.

Antonia and Luxton (1971) have observed developing boundary-layer velocity profiles of the form

$$\frac{u}{u_*} \propto z^{1/2} + \text{constant}. \tag{15}$$

4. Total Drag – Experimental

In relating the total-drag (11) to the experiments reviewed briefly in Section 2, it is necessary to test whether the plot of U/u_* versus $\ln(\delta/k\lambda\phi)$ can be represented adequately by a straight line, and to estimate a best value for the exponent β in (9).

Unavoidable differences occur in the experimental definitions of the quantities U and δ. Schlichting's experiments involved almost fully-developed, asymmetric duct

flows, U being taken as the maximum of the velocity profile. This occurs at a distance δ from the wall, where the mean shear stress changes sign. A corresponding point would be the free surface in the flume experiments of O'Loughlin and Macdonald. For the growing boundary layer in a wind tunnel (Moore, Marshall), δ represents the nominal boundary-layer thickness and U is the velocity of the uniform free stream. In the field experiments of Kutzbach and Bradley, however, the boundary layer due to the artificial roughness array grows in an already-established shear flow, so that the shear stress is finite at the top of the layer (Elliott, 1958; Panofsky and Townsend, 1964). It is usual to measure U and δ at the discontinuity on the mean-velocity profile where the slope changes from that of the growing shear layer to that of the established flow.

Initial attempts at fitting (11) were made using Marshall's data for cylinders, since this covered the widest range of parameter values. The mean boundary-layer thickness δ was not measured in all experiments, but was represented approximately by an empirical formula, based upon 7 experimental values,

$$\delta \approx 3.3 + 15.0\,(\lambda\phi)^{0.43} \quad [\mathrm{cm}].$$

The dependence upon $\lambda\phi$ arises because the roughness array modifies the thickness of its own boundary layer. The effect on δ of the coefficient β in (9), not determined at this stage, was found to be small.

A preliminary plot of Marshall's data for U/u_* versus $\log\lambda$ indicated a dependence analogous to that shown by $\ln(k_s/k)$ in Figure 1. With increasing $\ln\lambda$, U/u_* decreased steadily and linearly until partial sheltering of roughness elements occurred; the drag 'efficiency' then dropped, and U/u_* appeared to become stationary. At higher concentrations, U/u_* should obviously increase.

Attention is directed in Figure 3b, to Marshall's 22 data points (for $k/s = k/d$ lying between $\frac{1}{3}$ and 2) in the range $70 < \delta/k\lambda\phi < 2000$ where the conditions of the dimensional analysis appear to be applicable. (The elements of $k/s = \frac{1}{5}$ are excluded from this analysis for reasons given in Section 5). It had been found that for given β, the trend of U/u_* versus $\ln\lambda$ for particular k/s was linear, but displaced from the line for any other value of k/s. However, fitting a least-square straight line to all 22 points indicated a well-defined minimum in the residual sum of squares at $\beta \approx 0.38$ (Figure 2). With this value of β, which is adopted hereafter, the fit of a second-degree polynomial produces no significant reduction of the residual variance.

In Figure 3a, the straight line fitted to Marshall's data has the formula given in Table I (cf. Equation (11)), giving $\kappa \approx 0.25$. This unusually low value of κ may have something to do with the restricted size of the duct (cf. Section 2), relative to the element spacing D. Effects due to the proximity of the 4:1 tunnel contraction are not known. Nevertheless, the self-consistency of the data makes it useful for comparative studies with varying array geometry.

Some of Schlichting's (1936) results are also given in Figure 3a, with the results of least-square fitting in Table I. The most extensive data involve spheres of two sizes, for which $\kappa \approx 0.42$, close to the 'classical' value. For spherical segments, truncated

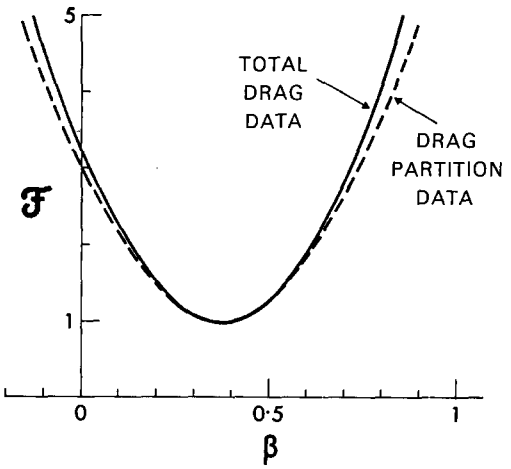

Fig. 2. Variation with respect to exponent β of the ratio $\mathcal{F}$ of residual variance to minimum variance in the least-square fit of straight lines to Marshall's (1970) data. Although a strict statistical '$\mathcal{F}$-test' cannot be applied, the figure shows that β is almost certainly positive.

cones and short transverse strips, the velocity profiles were steeper, with κ ranging from 0.33 to 0.37.

O'Loughlin and Macdonald (1964) obtained values of about 0.33 for κ from similar analyses using cube roughness elements in a wide range of concentrations. The data shown in Figure 3a and Table I are from O'Loughlin (1965). A considerable body of data for cubes was obtained by Koloseus and Davidian (1966) and is shown in Figure 3b.

The close grouping of the data for Schlichting's various shapes and for O'Loughlin's cubes, indicates that the shape description is adequate. A single straight line fitted to these 116 points has the coefficient values $C \approx -2.05$, $A \approx 2.865$ so that $\kappa \approx 0.35$. Recent very careful measurements of wind drag on a natural surface, wheat-crop stubble (Businger *et al.*, 1971), using both velocity-profile and drag-plate data, lead to the mean value $\kappa \approx 0.35$.

For measurements made in the atmosphere, the data in Figure 3a incorporate a -10% correction for the overspeeding of cup anemometers (Izumi and Barad, 1970). Kutzbach's data on arrays of bushel baskets exhibit a greater scatter than the laboratory results, but also fall in the same region of Figure 3a. The agreement between the different types of roughness element illustrated in Figure 3a is also remarkable because in several cases, values of k/s are involved which exceed $O(1)$. For the transverse strips used by Schlichting, $k/s \approx 10$. Bradley's (1965) values obtained with vertical round wires, for varying δ/k, are in good general agreement with the other results, although $k/s = k/d \approx 23$ – an extremely high value.

Several workers have investigated the flow over '2-dimensional' roughness elements consisting of transverse square bars with various spacing-to-chord ratios. Liu *et al.* (1966) varied this ratio over the range 1 to 24 and report a 'maximum roughness' in the region of 12. Koloseus and Davidian (1966) have collated other square-bar results

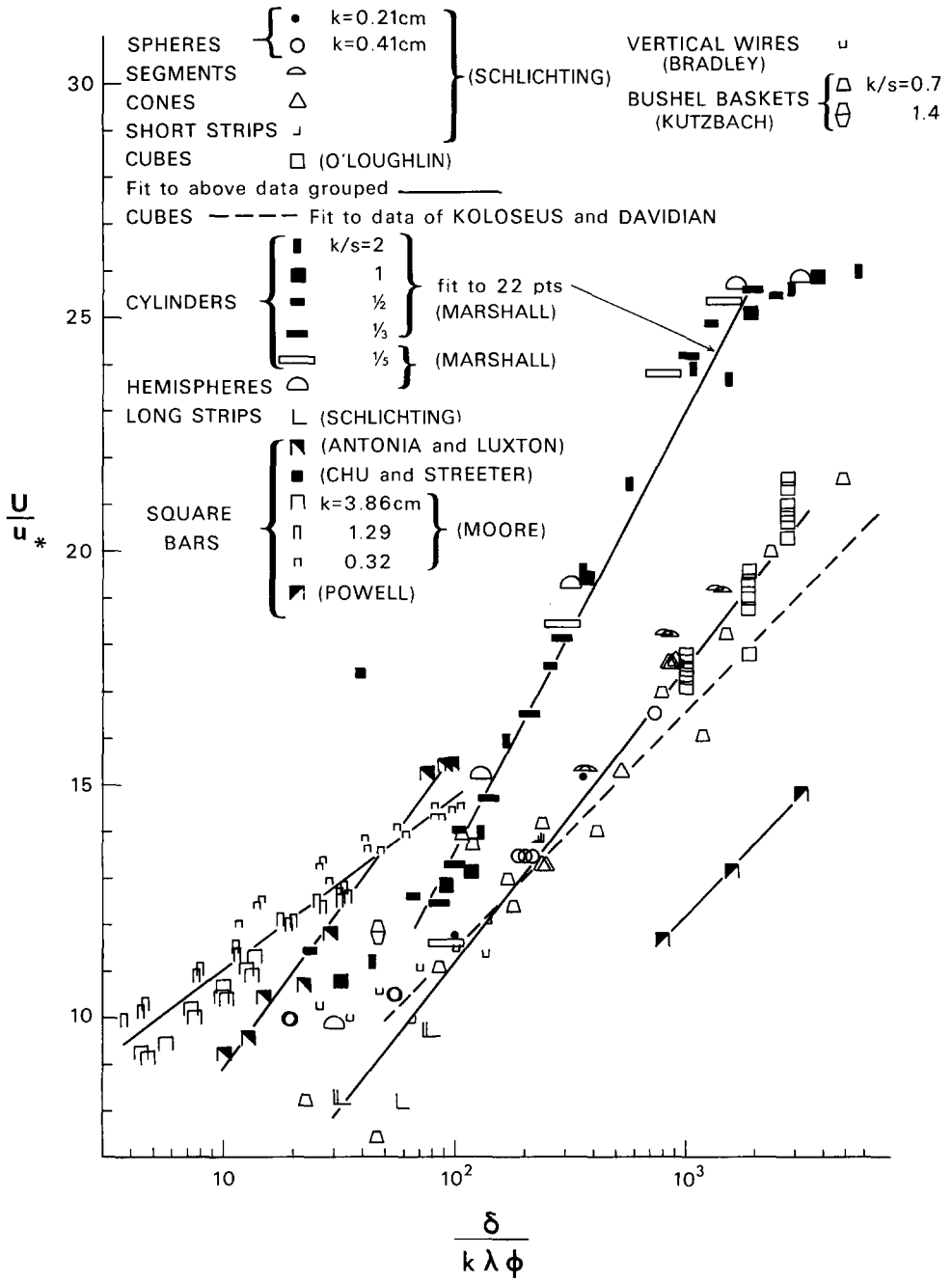

Fig. 3a. Measurements of total shear-stress plotted as U/u_* versus $\ln(\delta/k\lambda\phi)$ for the roughness configurations summarized in Table I.

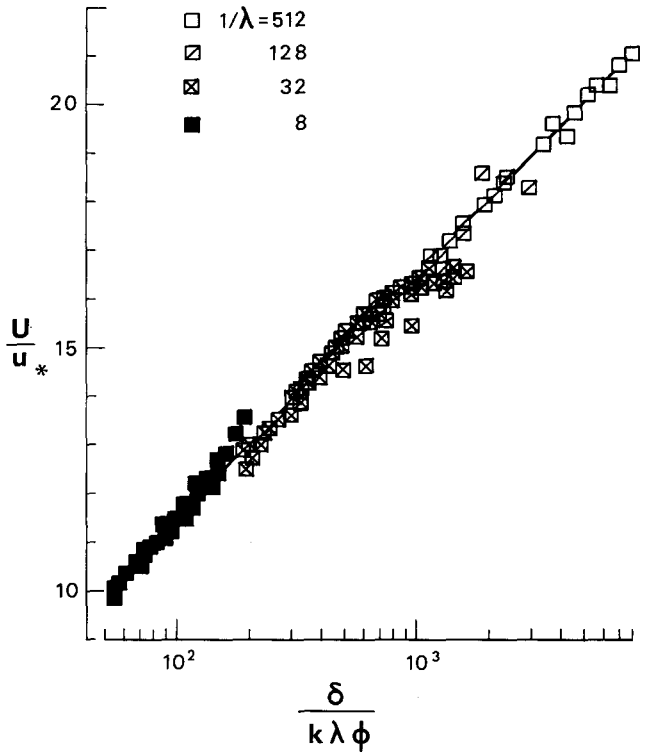

Fig. 3b. Data of Koloseus and Davidian (1966) for cubes in stable flow.

by Powell and by Chu and Streeter. Although Powell's data (included in Figure 3a) is of the 'k, D'-type, they fall separately from the discrete element data, indicating that (11) does not take complete account of the geometrical differences. The same is true of the single point from Chu and Streeter, which is probably close to the 'δ'-type roughness range.

Square-bar measurements in the 'k'-type roughness range are those of Moore (1951) and Antonia and Luxton (1971) in which the varying parameter is δ/k. Dependence on this parameter still appears to be logarithmic although the influence of roughness geometry is quite different, as noted above. Numerical constants for the square-bar data are included for completeness in Table I.

5. Drag Partition

5.1. Theory

Schlichting (1936) defined a roughness-element drag coefficient which will be re-written here as

$$C_f = \frac{w_r}{\frac{1}{2}\varrho u_k^2 A_r \phi} = \frac{w_r/S}{\frac{1}{2}\varrho u_k^2 \lambda \phi}, \tag{16}$$

where w_r is the mean drag per element, A_r is its frontal area and u_k is the velocity at the roughness height k above the plane supporting surface; i.e., from (10),

$$\frac{u_k}{u_*} = \frac{1}{\kappa} \ln \frac{1}{\lambda\phi} + C. \tag{17}$$

In general, C_f is not constant, being an unknown function of the roughness geometry. For an estimate of w_r/S, Schlichting applied the formula for drag partition

$$w_r/S = \varrho u_*^2 - \varrho u_{*g}^2 S'/S, \tag{18}$$

in which S' is that part of the specific area S which is not covered by the roughness element and u_{*g} is a mean shear velocity for the uncovered surface, dependent to some extent on the (finite) Reynolds number. However, Schlichting assumed that the second term on the right-hand side of (18) is frequently small compared with the first, and replaced u_{*g} by an average value ($=0.0461\bar{u}$) obtained from measurements using a smooth plate. The quantity $\bar{u}$ is the mean velocity in the shear layer, equal to $U-u_*/\kappa$ by integration of (7). In this way, values were obtained for C_f which tended to an upper limit as $\lambda \to 0$.

A weakness of Schlichting's approximation is the apparent dependence of u_{*g}/u_* upon U/u_*, implying that C_f is influenced by the outer region of the shear layer. More recently, O'Loughlin (1965) and O'Loughlin and Annambhotla (1969) have shown that for low roughness concentrations, the flow below the tops of the roughness elements is independent of the relative roughness δ/k, and so is governed by an 'inner law' (cf. Section 6). The simplest model based upon these experimental data, and valid as $\lambda \to 0$, is to assume that C_f is constant. Then the dependence of $(w_r/\varrho S)^{1/2}/u_*$ upon the roughness geometry follows from (16) and (17).

Einstein and Banks (1950) considered the partition of drag due to three sources on the bed of a flume: the bed itself, small transverse steps in the bed, and arrays of cylindrical pegs set into it. They arrived at an expression for the total drag by linear addition of the separate resistances from these three sources which were assumed to be mutually independent. Measurements over a range of fairly low concentration ($\lambda \approx 10^{-2}$ to 10^{-3}) enabled them to insert empirical constants in this expression.

5.2. Experimental observations

Marshall (1971) made direct measurements of drag on individual roughness elements within the array configurations described in Section 2. For the plot of the ratio $(w_r/\varrho S)^{1/2}/u_*$ versus $\ln(1/\lambda\phi)$, a straight line fitted to the 22 selected points again gives minimum residual variance for $\beta = 0.38$ (Figure 2). As before, a second-order polynomial reduces the residual variance by a negligible amount. The equation of the line has the form

$$(w_r/\varrho S)^{1/2}/u_* = A' \ln \frac{1}{\lambda\phi} + C' \tag{19}$$

with $A' = -0.179$ and $C' = 1.63$.

From O'Loughlin's (1965) data, the corresponding values are $A' = -0.093$ and $C' = 1.16$ for cube roughness elements.

Figure 4 illustrates these direct measurements, together with the fitted line (Equation (19)). However, an equally satisfactory fit to Marshall's data is afforded by Equations (16) and (17), assuming that $C_f = \text{constant} = 0.70$. As a comparison, $C_f \approx 1.2$ for O'Loughlin's cube data (cf. Roberson (1961)).

The graph indicates that the array $k/s = \frac{1}{5}$, does not group with the other data. A possible explanation is the breakdown of the 'aspect-ratio' relation $\phi = (k/s)^{\beta}$, since ϕ tends to a constant at small k/s (Tillmann, 1953, Figure 3; Marshall, 1971, Figure 5). The considerable surface area of the elements may also have produced skimming flow,

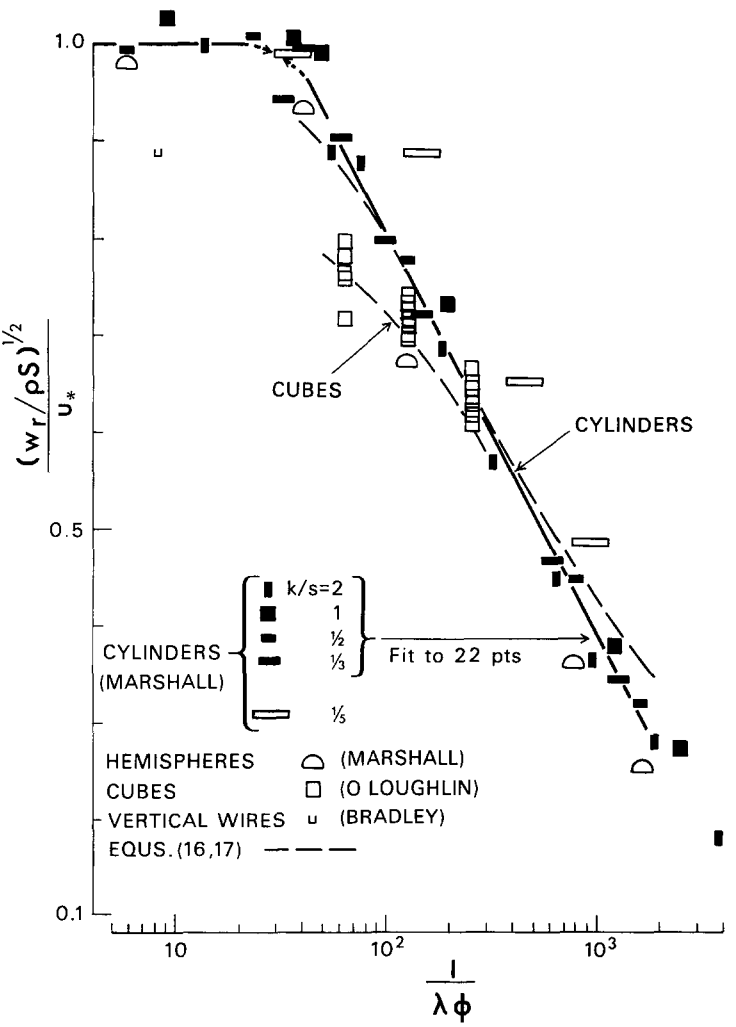

Fig. 4. Measurements of drag partition plotted as $(w_r/\varrho S)^{1/2}/u_*$ versus $\ln(1/\lambda\phi)$ for cylinders, hemispheres, cubes and vertical wires. (See Table I.)

a possibility supported by the slightly lower total drag observed (cf. Figure 3). An alternative possibility, the onset of a Reynolds-number transition arising from the large element diameter, must be ruled out since this would decrease rather than increase the ratio $(w_r/\varrho S)^{1/2}/u_*$.

6. Flow in the 'Wake Region'

O'Loughlin (1965) and O'Loughlin and Annambhotla (1969) refer to the region $z/k = O(1)$, extending below the tops of the roughness elements, as the 'wake layer'. In this region, the time-averaged flow tends to be three-dimensional in character, and a one-dimensional model can be only partially adequate. Oil-carbon streak photographs (cf. O'Loughlin, 1965) illustrate clearly the existence of a 'horse-shoe' vortex, with horizontal diameter of about $3k$, surrounding and streaming from each side of the roughness element. The formation of this vortex is partly an inviscid-flow phenomenon, and arises from the transfer of vorticity in the mean shear flow to vorticity in the streamwise direction (Squire and Winter, 1951; Hawthorne, 1951; Hawthorne and Martin, 1955).

For an isothermal incompressible inviscid fluid, one form of the Eulerian equations of motion is

$$\frac{\partial \mathbf{v}}{\partial t} + \tfrac{1}{2}\operatorname{grad} v^2 + \frac{1}{\varrho}\operatorname{grad} p = \mathbf{v} \times \boldsymbol{\omega}, \tag{20}$$

where $\mathbf{v}$ is the velocity vector, $\boldsymbol{\omega}$ $(=\operatorname{curl}\mathbf{v})$, is the vorticity, t is time, p is pressure and ϱ is the fluid density. The vector $\boldsymbol{\omega}$ can be decomposed into components parallel and normal to the flow. Taking the divergence of $\boldsymbol{\omega}$, using the conditions $\operatorname{div}\boldsymbol{\omega} = \operatorname{div}\mathbf{v} = 0$, gives

$$\mathbf{v}\cdot\operatorname{grad}(\omega_s/v) = \left[\mathbf{v}, \frac{1}{\varrho}\operatorname{grad}\left(\frac{1}{v^2}\right)\right] + \left[\mathbf{v}, \frac{\partial \mathbf{v}}{\partial t}, \operatorname{grad}\left(\frac{1}{v^2}\right)\right] \tag{21}$$

after elimination of $\mathbf{v}\times\boldsymbol{\omega}$, where each pair of square brackets signifies the scalar triple product of the enclosed vectors. This gives the spatial rate of increase of vorticity in the flow direction. In a 'steady' turbulent boundary layer, it is appropriate to take Reynolds variables $\mathbf{v} = \bar{\mathbf{v}} + \mathbf{v}'$, etc., where the bar signifies a time average and the prime a fluctuation from the average. Then, from the time average of (21)

$$\bar{\mathbf{v}}\operatorname{grad}\overline{(\omega_s/v)} = \left[\bar{\mathbf{v}}, \frac{1}{\varrho}\operatorname{grad}\bar{p}, \operatorname{grad}\overline{(1/v^2)}\right] + \text{cross-correlation terms.} \tag{22}$$

In an unobstructed part of a 'two-dimensional' turbulent boundary layer over a flat plate, $\operatorname{grad}\bar{p}$ is either zero or may have a component in the direction of $\bar{\mathbf{v}}$. Thus, the first term on the right-hand side of (22) is zero. The net effect of the cross-correlation terms is relatively small, being associated with a gradual increase in the thickness of the layer. However, the influence of an obstacle, such as a roughness element, is to introduce a spanwise component in $\operatorname{grad}\bar{p}$ which is not coplanar with $\bar{\mathbf{v}}$ and $\operatorname{grad}(\bar{v}^{-2}) = -(1/\bar{v}^4)\operatorname{grad}(v^{-2})$. Vorticity is then transferred from the mean shear

flow (where it is directed spanwise) to the direction of the flow. Viewed in the downstream direction, the rotation is anti-clockwise for flow passing to the right of a three-dimensional obstacle and clockwise for flow passing to the left. The directions of rotation are such as to transport high flow velocities downwards into the space behind the obstacle, which may create a slight velocity excess there (cf. Schlichting, 1936; Mons and Sforza, 1968).

Downstream of each roughness element, the break-up of the near-wake vortex contributes energy to the turbulent wake. This turbulence will be scaled to the dimensions of the roughness element, but will be modified at greater distances downstream to the scale of height above the intervening wall.

6.1. Mean-velocity measurements in and above the 'wake' region

Velocity-profile measurements for regular arrays of cube roughness elements, with roughness concentrations λ of $\frac{1}{64}$, $\frac{1}{128}$ and $\frac{1}{256}$ have been made by O'Loughlin (1965) and O'Loughlin and Annambhotla (1969). The most detailed results were obtained in a tilted flume with 0.95-cm elements at $\lambda = \frac{1}{64}$, the mean roughness Reynolds number being approximately 1100. These measurements which extended down to a dimensionless height of $z/k \approx 0.06$, were taken at a site from which a roughness element had been removed. To verify that such a procedure yielded profiles representative of the mean horizontal flow, O'Loughlin (1965) made supplementary measurements at several different sites. These indicated little change in profile except in the separation (near-wake) region close to each roughness element.

O'Loughlin and Annambhotla showed that the velocity profile was not dependent upon the ratio δ/k when the latter was reasonably large; i.e., the flow in the wake layer was determined by some kind of 'inner' law dictated by conditions near the boundary.

A replot of the flume data with $\lambda = \frac{1}{64}$ is given in Figure 5. This shows that the profile for $0.06 < z/k < 1$, can be represented empirically by the relation

$$\frac{u}{u_*} \approx 1.55 \ln \frac{z+b}{k} + 10.80, \tag{23}$$

where $b/k \approx 0.15$. By contrast, the profile for $z/k > 2$ gives

$$u/u_* \approx 2.50 \ln (z/k) + 10.80. \tag{24}$$

Evidently κ is very close to 0.4 in this particular case.

Equation (23) is merely a convenient fit to experimental data, but it does suggest that the shear velocity does not vary greatly with height in a significant part of the range $0 \leqslant z/k < 1$. This is not unreasonable since, for $\lambda = \frac{1}{64}$, the roughness-element spacing is at least 8 times the roughness height k, and in the above height range, the distance to the intervening surface is usually much less than to neighbouring roughness elements. If the form of (23) is assumed to be the same as that of (24), with the same value of κ, a comparison of the two equations gives $u_{*g}/u_* \approx 1.55/2.5 \approx 0.62$, where

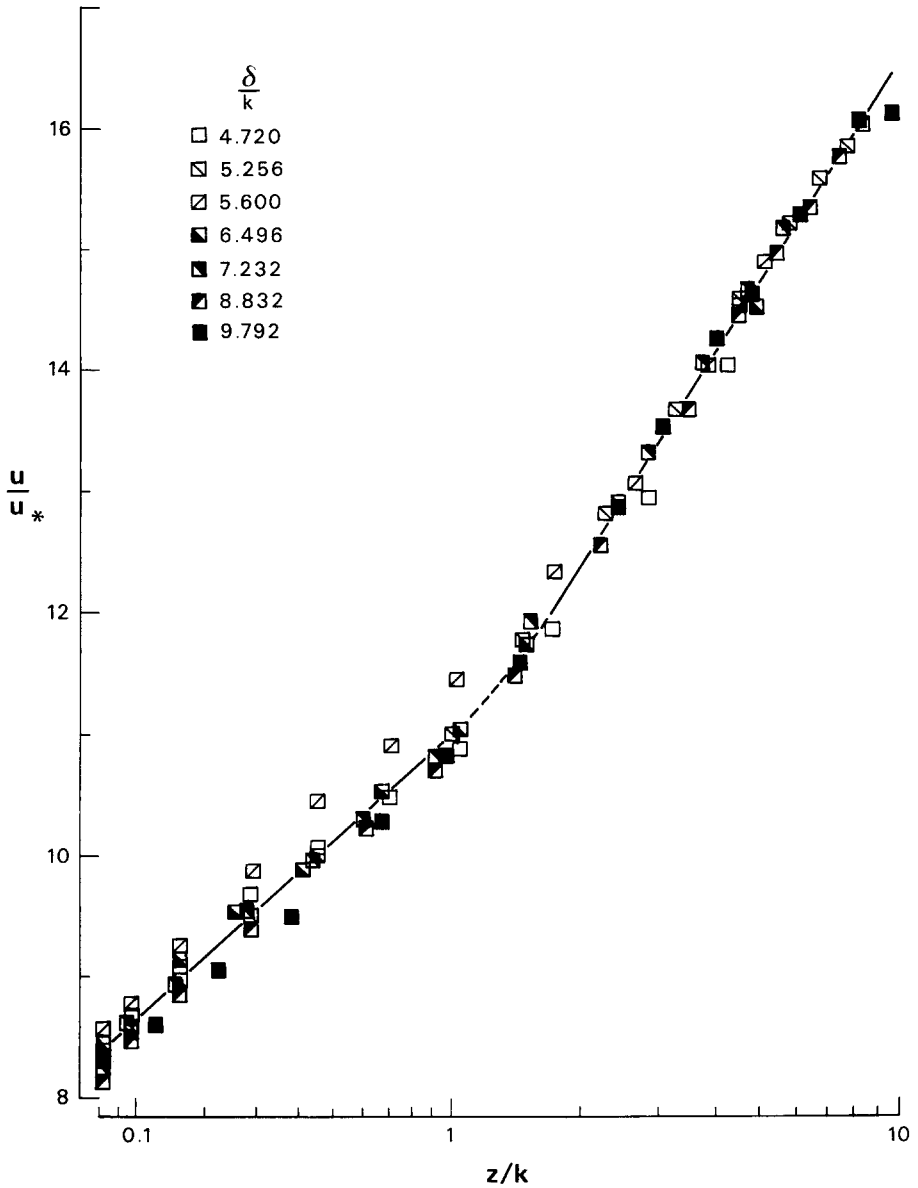

Fig. 5. Velocity-profile measurements (O'Loughlin and Annambhotla, 1969) u/u_* versus distances proportional to $\ln(z/k + 0.15)$ for a cube array with concentration $\lambda = 1/64$.

u_{*g} is the shear velocity at the intervening surface. Thus about 60% of the total stress arises from drag upon the roughness elements.

From (23) and the definition of u_{*g}, it is possible to write an empirical expression for the momentum-diffusion coefficient K_M:

$$K_M \approx \kappa u_{*g}(z + b). \tag{25}$$

The presence of the height z indicates the importance of the distance from the intervening smooth wall. However, turbulent mixing is enhanced by the wakes of the roughness elements which contribute a positive term $\kappa u_{*g} b$ to the momentum-diffusion coefficient, where b is scaled to the roughness geometry for which k is an appropriate reference length. The observed small value of the ratio b/k (in spite of the high roughness-element drag) may be due to a reduction in eddy scale as the near-wake vortex is extended in the downstream direction.

6.2. Uniformly valid representation

Any number of empirical formulae might be found which represent the data of Figure 5 adequately over the experimental range. If (23) and (24) are regarded as asymptotic expressions, valid for $z/k \to 0$ (excluding the viscous sublayer) and $z/k \to \infty$, respectively, a representation which holds in the same manner at both ends of the range might be termed uniformly valid. The expression

$$\frac{u}{u_*} \approx \frac{1}{\kappa}\left\{\frac{u_{*g}}{u_*} + \left(1 - \frac{u_{*g}}{u_*}\right) e^{-k/z}\right\} \ln \frac{z+b}{k} + C \tag{26}$$

is a simple and effective choice, involving no additional parameters. For $\kappa \approx 0.4$, $b/k \approx 0.15$, $C \approx 10.8$ and $u_{*g}/u_* \approx 0.62$, (26) follows very closely the curve of best fit shown in Figure 5.

Presumably b is a function of the spacing D of the roughness elements, but there are no data available to establish the dependence with any certainty. From dimensional considerations, the relation $b/k \approx 1.2k/D$ appears reasonable for cube roughness elements, where the coefficient may be related to the drag coefficient C_f (see Section 5).

6.3. Viscous sublayer

The representations (23) and (26) are not valid close to the intervening surface as the viscous region is approached. Following O'Loughlin and Annambhotla (1969), let the smooth-wall sublayer thickness δ_s be scaled by a limiting Reynolds number $M = u_{*g}\delta_s/\nu$ and, within the viscous sublayer, put $u_{*g}^2 = \nu u/\delta_s$ approximately, where u_s is the velocity at the outer edge of the sublayer. From these relations, $u_s/u_* = M u_{*g}/u_*$, while, by extrapolation of (23) down to the wall,

$$u_s/u_* \approx 1.55 \ln(0.15) + 10.80 \approx 7.86 .$$

With $u_{*g}/u_* \approx 0.62$, these give $M \approx 12.7$, which is not significantly different from the average value of 12.2 found by O'Loughlin using a different profile assumption. These results are in good agreement with the measurements of other workers in the viscous sublayer over a smooth plate. See, for example, the data collated by Thwaites (1960, p. 58).

7. Conclusions

It has been demonstrated that the aerodynamic resistance of a surface covered with discrete roughness elements in a regular pattern may be described by universal laws

involving the geometry of the rough surface, and the nature of the boundary layer associated with it.

The dimensionless groupings which characterize the roughness are the 'concentration' ratio, element frontal area/surface area per element (A_r/S), and an element 'shape factor', height/thickness (k/s). These are found to combine as

$$\frac{A_r}{S}\cdot\left[\frac{k}{s}\right]^{0.4} \equiv \lambda\phi\,.$$

The scaling parameters for the boundary layer are its thickness δ (where velocity $= U$) and the shear velocity u_*. The resulting drag law

$$\frac{U}{u_*} = 2.87 \ln \frac{\delta}{k\lambda\phi} - 2.05 \qquad (27) \quad \text{(from 11)}$$

is valid over a range $30 < \delta/k\lambda\phi < 2000$ in which the total resistance is partitioned between bluff body drag on the obstacles, and shear on the intervening floor, i.e., it is influenced by both the obstacle height and spacing, and has thus been designated the 'k, D'-roughness regime (Figure 1). Within this regime, Equation (27) is supported by experimental data from a variety of obstacle shapes and flow conditions. Data which do not conform to the universal function (27) are those for long bars laid across the width of the flow section. This form of roughness, used by many workers, may possibly be regarded as a one-dimensional horizontal pattern in contrast with the two-dimensional pattern which the geometrical ratios A_r/S and k/s characterize successfully. Furthermore, bar data from several sources encompassing the three proposed concentration regimes 'k, D', 'k' and 'δ', demonstrate in Figure 3a that the resistance law is strongly 'regime-dependent'.

The constant 2.87 in (27) is identified with the reciprocal of the von Karman constant κ, implying therefore a value of κ close to 0.35. It should be pointed out, however, that the data have been adopted uncritically for the purpose of the least-square fit and serve primarily to caution that the magnitude and the constancy of von Karman's 'constant' has yet to be established.

The proportion of total drag dissipated as bluff body forces on the obstacles may also be represented in terms of the geometrical group $\lambda\phi$. If the force per element w_r is expressed as a proportion of the total shear stress, the limited amount of relevant data supports an empirical drag partition equation of the form

$$(w_r/\varrho S)^{1/2}/u_* = A' \ln \frac{1}{\lambda\phi} + C'\,,$$

valid as before, over the regime of 'k, D'-roughness.

An alternative approach specifies the force on an element in terms of a drag coefficient referred to the wind speed at the top of the elements

$$C_f = (w_r/S\lambda\phi)/\tfrac{1}{2}\varrho u_k^2\,.$$

Use can be made of this definition with the aid of two assumptions; that C_f is roughly

constant for a given species of element over a significant range as $\lambda \to 0$ and that Equation (10) is valid at $z = k$. Figure 4 demonstrates good agreement between the drag partition calculated in this way for arrays of cylinders and cubes. For practical purposes this procedure may provide a reasonable estimate of the drag on individuals in an obstacle array, provided that their shapes and appropriate C_f' s can be specified.

The mechanism through which the wakes from individual elements interact with the flow around and between them can be analysed in terms of a transformation of shear-induced vorticity in what has been termed the 'wake layer'. The concept, for 'k, D'-distributions, of positive and essentially uniform drag over the majority of the intervening surface, leads to a coherent description of flow in the wake layer. Data for an array of cubes yield a logarithmic velocity profile when the height scale is augmented by a small factor b/k, where b is presumed to be a function of the array geometry. From this profile may be deduced the shearing stress u_{*g} appropriate to the intervening surface and a turbulent momentum diffusion coefficient which includes a small quantity $\kappa u_{*g} b$ which, it is proposed, is the contribution from element wakes. A single expression has also been found, to represent this velocity data continuously through both the wake and boundary layers.

When the surface stress is combined, through the wake-layer profile, with an assumed linear velocity gradient u_s/δ_s across the viscous sublayer, the quantity $u_{*g}\delta_s/\nu = 12.7$. This is very close to values reported for the viscous sublayer over an *unobstructed* smooth plate.

The above analysis arose from such environmental problems as soil erosion and wind sheltering where the drag forces on shrubs and the bare ground between them is an important factor. In fact, the configurations which have been considered here occur rather frequently on the earth's surface, in forest plantations, orchards, young crops and the arrays of cubes in suburbia.

Apart from the variability of natural wind, and the added complication on most occasions caused by a convective component of turbulence, the most notable difference between these examples and the data considered in this paper is that of length scale. The most careful and detailed measurements available are obviously those made with laboratory techniques and to obtain results of comparable accuracy in the atmosphere is extremely difficult. However, successful accommodation into the framework outlined here of the few atmospheric results, should encourage micrometeorologists to attempt further measurements of drag partition and velocity distribution in the vicinity of objects on the earth's surface.

Acknowledgments

The authors gratefully acknowledge the benefit of valuable discussions with Dr E.M. O'Loughlin, who generously made available the original expermental data from which the constants in Equations (23) and (24) were calculated and Figure 5 was plotted. Dr O'Loughlin also provided the data on cube roughness plotted in Figures 3a and 4.

The above work was completed while the first author was visiting the Department of Geography and Environmental Engineering of The Johns Hopkins University.

References

Antonia, R. A. and Luxton, R. E.: 1971, 'The Response of a Turbulent Boundary Layer to a Step Change in Surface Roughness'. Part 1 'Smooth to Rough', *J. Fluid Mech.* **48**, 721–61.

Bradley, E. F.: 1965, 'Studies of Wind Drag on the Earth', Ph. D. thesis, Australian National University.

Bradley, E. F.: 1968, 'A Micrometeorological Study of Velocity Profiles and Surface Drag in the Region Modified by a Change in Surface Roughness', *Quart. J. Roy. Meteorol. Soc.* **94**, 361–79.

Businger, J. A., Wyngaard, J. C., Izumi, Y., and Bradley, E. F.: 1971, 'Flux-Profile Relationships in the Atmospheric Surface Layer', *J. Atmos. Sci.* **28**, 181–89.

Clauser, F. H.: 1956, 'The Turbulent Boundary Layer', *Adv. Appl. Mech.* **4**, 1–51.

Coles, D.: 1956, 'The Law of the Wake in the Turbulent Boundary Layer', *J. Fluid Mech.* **1**, 191–226.

Corrsin, S. and Kistler, A. L.: 1955, 'Free-Stream Boundaries of Turbulent Flows', NACA Rep. 1244.

Dryden, H. L.: 1953, 'Review of Published Data on the Effect of Roughness on Transition from Laminar to Turbulent Flow', *J. Aero. Sci.* **20**, 477–82.

Einstein, H. A. and Banks, R. B.: 1950, 'Fluid Resistance of Composite Roughness'. *Trans. Am. Geophys. Union* **31**, 603–10.

Elliott, W. P.: 1958, 'The Growth of the Atmospheric Internal Boundary Layer', *Trans. Am. Geophys. Union* **39**, 1048–54.

Hawthorne, W. R.: 1951, 'Secondary Circulation in Fluid Flow', *Proc. Roy. Soc.* A **206**, 374–87.

Hawthorne, W. R. and Martin, M. E.: 1955, 'The Effect of Density Gradient and Shear on the Flow over a Hemisphere', *Proc. Roy. Soc.* A **232**, 184–95.

Izumi, Y. and Barad, M. L.: 1970, 'Wind Speeds as Measured by Cup and Sonic Anemometers and Influenced by Tower Structure', *J. Appl. Meteorol.* **9**, 851–56.

Koloseus, H. J. and Davidian, J.: 1966, 'Free-Surface Instability Correlations, and Roughness-Concentration Effects on Flow over Hydrodynamically-Rough Surfaces', USGS Water-Supply Paper 1592-C, D.

Kutzbach, J. E.: 1961, 'Investigations of the Modification of Wind Profiles by Artificially Controlled Surface Roughness', Univ. of Wisconsin, Dept. of Meteorol., Annual Report, pp. 71–113.

Lettau, H. H.: 1967, 'Problems of Micrometeorological Measurements', in E. F. Bradley and O. T. Denmead (eds.), *The Collection and Processing of Field Data*, Interscience, New York, pp. 3–40.

Lettau, H. H.: 1969, 'Note on Aerodynamic Roughness-Parameter Estimation on the Basis of Roughness-Element Description', *J. Appl. Meteorol.* **8**, 828–32.

Liu, C. K., Kline, S. J., and Johnson, J. P.: 1966, 'An Experimental Study of Turbulent Boundary Layer on a Rough Wall', Thermosciences Div., Mech. Eng. Dept., Report MD-15, Stanford University.

Marshall, J. K.: 1970, 'Assessing the Protective Role of Shrub-Dominated Range-Land Vegetation Against Soil Erosion by Wind', *Proc. Intern. Grassland Congr.*, Surfers Paradise, **11**, 19–23.

Marshall, J. K.: 1971, 'Drag Measurements in Roughness Arrays of Varying Density and Distribution', *Agric. Meteorol.* **8**, 269–92.

Millikan, C. B.: 1938, 'A Critical Discussion of Turbulent Flows in Channels and Circular Pipes', *Proc. 5th Intern. Congr. Appl. Mech.*, Cambridge, Mass., pp. 386–92.

Mons, R. F. and Sforza, P. M.: 1968, 'The Three-Dimensional Wake Behind an Obstacle on a Flat Plate', Polytech. Inst. of Brooklyn, PIBAL Rep. No. 68–20.

Moore, W. L.: 1951, 'An Experimental Investigation of the Boundary-Layer Development Along a Rough Surface', Ph. D. Dissertation, University of Iowa.

Morris, H. M.: 1955, 'A New Concept of Flow in Rough Conduits', *Trans. Am. Soc. Civil Engrs.* **120**, 373–98.

Nikuradse, J.: 1933, 'Strömungsgesetze in rauhen Rohren', *Forschungshefte* **361**, VDI; NACA Tech. Mem. 1292, 1950.

O'Loughlin, E. M.: 1965, 'Resistance to Flow over Boundaries with Small Roughness Concentrations', Ph. D. Dissertation, University of Iowa.

O'Loughlin, E. M. and Annambhotla, V.S.S.: 1969, 'Flow Phenomena near Rough Boundaries', *J. Hydraul. Res.* **7**, 231–50.

O'Loughlin, E. M. and Macdonald, E. G.: 1964, 'Some Roughness-Concentration Effects on Boundary Resistance', *La Houille Blanche* **19**, 773–82.

Panofsky, H. A. and Townsend, A. A.: 1964, 'Change of Terrain Roughness and the Wind Profile', *Quart. J. Roy. Meteorol. Soc.* **90**, 147–55.

Perry, A. E., Schofield, W. H., and Joubert, P. N.: 1969, 'Rough Wall Turbulent Boundary Layers' *J. Fluid Mech.* **37**, 383–413.

Roberson, J. A.: 1961, 'Surface Resistance as a Function of the Concentration and Size of Roughness Elements', Ph. D. Dissertation, University of Iowa.

Roberson, J. A.: 1968, 'Surface Resistance of Plane Boundaries Roughened with Discrete Geometric Shapes', Bull. 308, College of Engineering, Washington State University.

Roberson, J. A. and Chen, C. K.: 1970, 'Flow in Conduits with Low Roughness Concentration', *J. Hydraul. Div. ASCE* **96**, 941–57.

Rouse, H. (ed): 1959, *Advanced Mechanics of Fluids*, Wiley, New York.

Sayre, W. W. and Albertson, M. L.: 1961, 'Roughness Spacing in Rigid Open Channels', *Proc. Am. Soc. Civil Engrs, Hydraul. Div.* **87**, 121–50.

Schlichting, H.: 1936, 'Experimentelle Untersuchungen zum Rauhigkeitsproblem', *Ing.-Arch.* **7**, 1–34; NACA Tech. Mem. 823.

Squire, H. B. and Winter, K. G.: 1951, 'The Secondary Flow in a Cascade of Airfoils in a Nonuniform Stream', *J. Aero. Sci.* **18**, 271–77.

Tani, I.: 1961, 'Effect of Two-Dimensional and Isolated Roughness on Laminar Flow', in *Boundary Layer and Flow Control*, Pergamon Press, Oxford, pp. 637–56.

Thwaites, B.: 1960, *Incompressible Aerodynamics*, Oxford University Press.

Tillmann, W.: 1953, 'Neue Widerstandsmessungen an Oberflächenstörungen in der turbulenten Reibungsschicht', *Forschungshefte Schiffstechnik* **1**, 81–88.

Von Karman, Th.: 1934, 'Turbulence and Skin Friction', *J. Aero. Sci.* **1**, 1–20.

Wieghardt, K.: 1953, 'Erhöhung des turbulenten Reibungswiderstandes durch Oberflächenstörungen', *Forschungshefte Schiffstechnik* **1**, 65–81.